

## Lateral confining action of mortar-filled sleeve reinforcement splice

Hyong-Kee Kim\*<sup>1</sup> and Sang-Ho Lee<sup>2a</sup>

<sup>1</sup>Department of Architectural Engineering, Kangwon National University,  
346 Joongang-ro, Samcheok, Gangwon-do, Korea

<sup>2</sup>Department of Architectural Engineering, Hanzhong University,  
200 Jiyang-gil, Donghae, Gangwon-do, Korea

(Received December 22, 2010, Revised January 5, 2012, Accepted January 10, 2012)

**Abstract.** Of the various methods of splicing reinforcing bar in reinforced concrete structure, mortar-filled sleeve reinforcement splice offers diverse benefits, not only in terms of structural performance but also for the construction process. Consequently, after the mortar-filled sleeve splices have been developed in recent years, research and development on these splices has been actively carried out, in order to evaluate its macro structural performance, such as its strength and stiffness, with the aim of enabling this system to be applied to construction in the field as early as possible. However, to make a proper evaluation on the overall structural performance of the mortar-filled sleeve reinforcing bar splice, it is of critical importance to understand the lateral confining action of the sleeve, which is known to affect the bond strength between the embedded bar and mortar in the sleeve. Accordingly, in this study, an experiment of monotonic loading and cyclic loading was conducted with a full-sized mortar-filled sleeve splice attaching strain gauges on the sleeve surface with experimental variables such as development length of bar, etc. Based on the test results, the effect of the lateral confining action of the sleeve was analyzed and considered in terms of the bond strength between the bar and mortar in this splice.

**Keywords:** lateral confining action; mortar-filled sleeve reinforcing bar splice; bond strength; confining pressure; development length

---

### 1. Introduction

Of the various methods used to splice between reinforcement in reinforced concrete structure, the mortar-filled sleeve reinforcing bar splice, one of the mechanical splicing methods, is being very effectively applied in the field because it secures the required structural performance, good workability, and can be applied to large-diameter bar, the use of which is currently increasing. With its diverse benefits, and since the mortar-filled sleeve splices have been developed, active experimental studies have been carried out to evaluate structural performance such as the strength and stiffness of this splice (Einea *et al.* 1995, Ase *et al.* 1996, Kim 2008), to enable this system to be applied to building construction as early as possible. But, it is also very important to understand

---

\*Corresponding author, Associate Professor, E-mail: [hyongkee@kangwon.ac.kr](mailto:hyongkee@kangwon.ac.kr)

<sup>a</sup>Associate Professor, E-mail: [sangho@hanzhong.ac.kr](mailto:sangho@hanzhong.ac.kr)

the lateral confining action of the sleeve, which is known to affect bond strength between the embedded bar and mortar in the sleeve, in order to make a proper evaluation on the overall structural performance of the mortar-filled sleeve bar splice.

Until now, studies on the confinement action of a structure were mainly focused on the structural members such as columns or girders, on which axial load or bending moment acts. Of these, studies on confinement action of concrete-filled tube (CFT) column, which has gradually grown in popularity, have been carried out actively in diverse areas, such as studies for establishment of a structural design method of CFT columns (Kilpatrick and Rangan 1999, Liu and Ghossein 2005, Liu 2006, Lue *et al.* 2007, Choi *et al.* 2008, Liang 2009) and studies regarding the structural performance of CFT columns confined by carbon fiber reinforced polymer (Xiao *et al.* 2005, Tao *et al.* 2007, Park *et al.* 2010). For reinforced concrete structures, experiments and analyses were carried out with a focus on the study of the structural characteristics of concrete confined by transverse reinforcement (Mander *et al.* 1988, Saatcioglu and Razvi 1992, Cusson and Paultre 1994, Saadatmanesh *et al.* 1994, Cusson and Paultre 1995, Mirmiran and Shahawy 1997, Saatcioglu and Razvi 1998, Razvi and Saatcioglu 1999, Bing *et al.* 2001). Furthermore, studies have been continuously carried out on the influence of confining action against concrete on bond strength between deformed bar and concrete (Orangun *et al.* 1977, Soroushian *et al.* 1991). Consequently, it is widely known that the confining pressure of the concrete increases the bond strength between the reinforcing bar and its surrounding concrete. However, in reality there has been nearly no research that has aimed to understand the confinement action which affects bond strength between the single bar and its surrounding filling material, such as for the mortar-filled sleeve splice. Untrauer and Henry (1965) performed the pull-out test with reinforced concrete applying lateral confining pressure, and identified a relationship between the bond strength of deformed bar to its surrounding concrete and lateral confining pressure.

Einea *et al.* (1995) tried to evaluate the influence of the confinement action of steel pipe on the bond strength between the reinforcing bar and its surrounding mortar after conducting an experiment of monotonic loading with a mortar-filled steel pipe splice embedding D16 and D19 bar. While Einea's study showed the confining pressure of the steel pipe acting on the splice from the result of strain gauges attached on two specimens, it was less accurate in determining the confinement pressure of sleeve, as there was a lack of consideration of Poisson's effect, which occurs in the sleeve. Ahn *et al.* (2003) showed the confining pressure that acts on three specimens through monotonic loading test after producing a mortar-filled cast sleeve splice embedding D19 and D25 bar. In addition, the author of this study (2008) studied confinement action acting on mortar-filled steel pipe splice through monotonic and cyclic loading test in order to identify the confining effect of the mortar-filled steel pipe splice after producing experimental specimens using D25 and D32 bar.

As seen above, studies on the confining action of the mortar-filled sleeve bar splice have been limited mainly to monotonic loading test using small-diameter bar, or to steel pipe splice even for the cyclic loading test using large-diameter bar, which shows that details of those experimental studies are not sufficient. As such, more experimental studies with various variables shall be required for a more accurate evaluation on the confinement action by the sleeve in the mortar-filled sleeve bar splice.

Thus, in this study, we analyzed and studied the effect of the lateral confinement action by sleeve on the bond strength between bar and its surrounding mortar from an experimental result of this bar splice after conducting an experiment with the sleeve splice embedding SD500 bar made of ductile

cast iron, which allows more freely-shaped sleeves with variables of development length of bar and loading methods, etc.

## 2. Experiment

### 2.1 Planning and production of the specimen

Variables of this study are as follows.

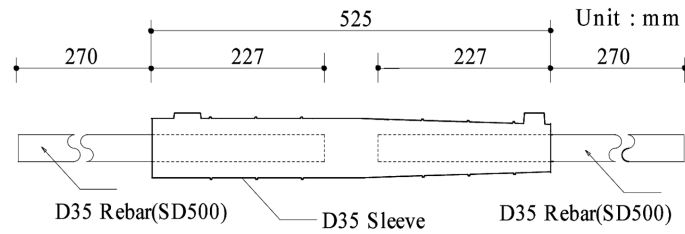
1. Development length of the bar embedded in the sleeve,  $L_d$  ( $L_d = 6.5d$ ,  $L_d = 5d$ ,  $L_d = 4d$ , where  $d$  is nominal diameter of the bar)
2. Size of the bar embedded in the sleeve (D25, D35)
3. Compressive strength of the mortar filled in the sleeve (Specified compressive strength is 75 MPa, 95 MPa for 28 days)
4. Loading methods (Monotonic loading, Cyclic loading)

As shown in Table 1, eight full-sized specimens were produced considering the above variables. Shapes of representative specimens and details of the sleeve for D35 bar are illustrated in Fig. 1 and Fig. 2. The Post Grout method was selected to fill mortar in sleeve of specimens, and mortar was filled from the lower entrance of sleeve while keeping it standing vertically and upright using a device developed to fix the sleeve. Mixing ratio between the water and mortar was 15%, and mixing time was approximately 2 minutes. A pump for filling mortar in the construction site was used to fill mortar. Two-direction strain gauges were attached at designated locations on the surfaces of eight experimental specimens in order to measure longitudinal and tangential strain in the sleeve. Fig. 3 shows the locations of strain gauges attached to the sleeves of a representative splice

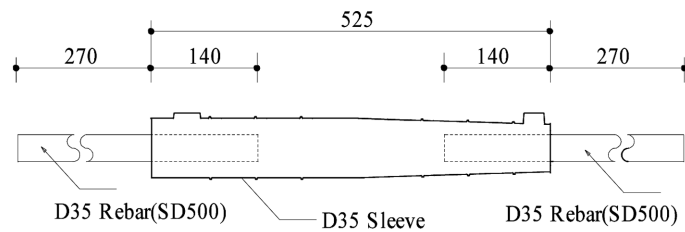
Table 1 List of experimental specimens

No.	Specimen name	Experimental variables			
		$L_d^{*1}$ (d)	Bar size	$f_m^{*2}$ (MPa)	Loading method <sup>*3</sup>
1	1122NM-1 <sup>*4</sup>	6.5	D25 <sup>*7</sup>	75	M
2	1322NM-1 <sup>*4</sup>	6.5	D35 <sup>*8</sup>	75	M
3	1322NC-1 <sup>*5</sup>	6.5	D35 <sup>*8</sup>	75	C
4	1322HM-1 <sup>*6</sup>	6.5	D35 <sup>*8</sup>	95	M
5	1344NM-1 <sup>*4</sup>	5.0	D35 <sup>*8</sup>	75	M
6	1344NC-1 <sup>*5</sup>	5.0	D35 <sup>*8</sup>	75	C
7	1355NM-1 <sup>*4</sup>	4.0	D35 <sup>*8</sup>	75	M
8	1355NC-1 <sup>*5</sup>	4.0	D35 <sup>*8</sup>	75	C

**Note** <sup>\*1</sup>: Development length of bar, <sup>\*2</sup>: Specified compressive strength of Mortar, <sup>\*3</sup>: M = Monotonic loading, C = Cyclic loading, <sup>\*4</sup>: NM means that mortar with normal strength ( $f_m = 75$  MPa) was used for the specimen and monotonic loading was performed on it, <sup>\*5</sup>: NC means that mortar with normal strength ( $f_m = 75$  MPa) was used for the specimen and cyclic loading was performed on it, <sup>\*6</sup>: HM means that mortar with high strength ( $f_m = 95$  MPa) was used for the specimen and monotonic loading was performed on it, <sup>\*7</sup>: D25 (Nominal diameter = 25.4 mm), <sup>\*8</sup>: D35 (Nominal diameter = 34.9 mm)



(a) Specimen 1322NM-1, 1322NC-1, 1322HM-1



(b) Specimen 1355NM-1, 1355NC-1

**Note** D35(Nominal diameter=34.9mm),  
SD500(Specified yield strength=491MPa)

Fig. 1 Shapes of representative specimens

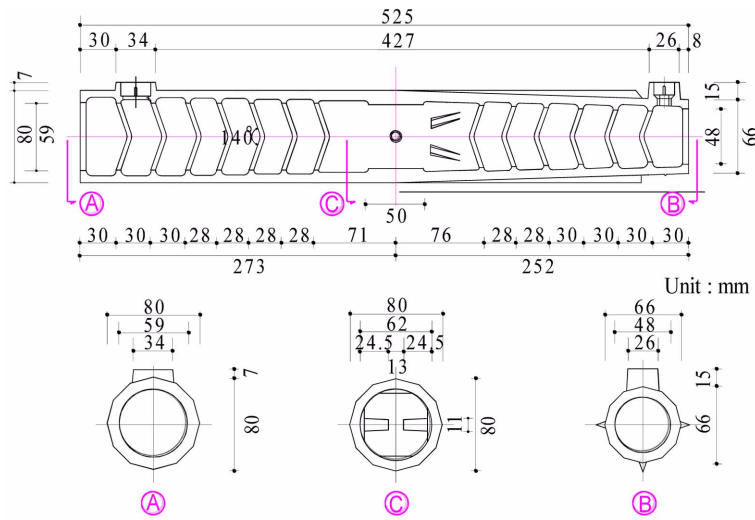


Fig. 2 Details of sleeve for D35 bar

specimen. As shown in Fig. 3, installation work of strain gauges was performed after completing filling mortar and curing.

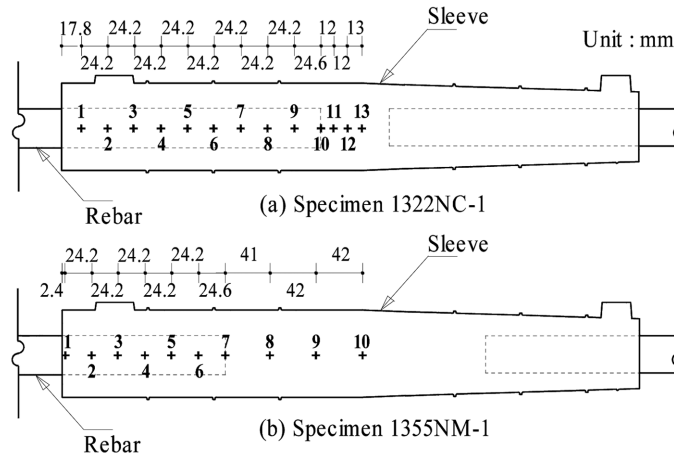


Fig. 3 Location of strain gauge attachment on sleeve surface of representative specimens

2.2 Mechanical properties of materials

D25 and D32 reinforcing bar of SD500 were used in this experiment. Test result of tensile strength on these bars is shown in Table 2. The sleeve material used in the experiment is ductile cast iron, and test result of tensile strength on this sleeve material is provided in Table 3. Two types of non-shrink mortar were used in experimental specimens, one of which had been previously developed while the other was newly developed to enhance compression strength. Compression test of mortar was implemented according to ASTM C 109 using 50 mm × 50 mm × 50 mm cubic specimen. Table 4 shows the test result of the compression strength on mortar.

Table 2 Test results of tensile strength of reinforcing bar

Bar size	Yield strength (MPa)	Tensile strength (MPa)	Elongation ratio (%)
D25	529	641	16.8
D35	545	712	17.3

Table 3 Test results of tensile strength of sleeve material

Yield strength (MPa)	Tensile strength (MPa)	Elongation ratio (%)
428	674	7.0

Table 4 Test results of compressive strength of non-shrink mortar

Mortar type	Compressive strength (MPa)
N mortar <sup>*1</sup>	87.5
H mortar <sup>*2</sup>	99.7

**Note** <sup>\*1</sup> : Existing mortar made exclusively for filling in sleeve, with a specified compressive strength of 75 MPa.  
<sup>\*2</sup> : Mortar developed to enhance the compressive strength of existing mortar, with a specified compressive strength of 95 MPa.

### 2.3 Loading and measuring methods

In this test, loading was performed by using 2,000 kN Universal Testing Machine, as is shown in Fig. 4. Monotonic loading was carried out until a failure occurred on the specimen by gradually increasing tensile load after gradually increasing the load until the tensile stress became 95% of the specified yield strength of bar embedded in the sleeve and removing this load. For cyclic loading, after repeatedly and gradually increasing load on the specimen 30 times until the tensile stress reaches 95% of the specified yield strength, and down to 2%, the specimen was finally destroyed by loading tensile force.

Longitudinal and tangential strain was measured together with the load applied on the specimen in this test.

### 2.4 Result of the experiment

Maximum strength and final failure mode of eight specimens are shown in Table 5, where the maximum strength of the specimen is obtained from dividing the maximum load on the specimen by the nominal sectional area of reinforcing bar. Final failure figures of representative specimens 1322NC-1 (development length of bar is 6.5d, cyclic loading and bar fracture) and 1355NM-1 (development length of bar is 4d, monotonic loading and bond failure) are shown in Figs. 5 and 6. Figs. 7 and 8 indicate longitudinal and tangential strain of the two representative specimens above.



Fig. 4 Specimen setup

Table 5 Result of experiment

Specimen	Tensile strength (MPa)	Final failure mode <sup>*1</sup>
1122NM-1	642	R
1322NM-1	711	R
1322NC-1	709	R
1322HM-1	707	R
1344NM-1	709	B
1344NC-1	709	B
1355NM-1	645	B
1355NC-1	635	B

Note <sup>\*1</sup>: R = Reinforcing bar fracture, B = Bond failure



Fig. 5 Final failure pattern (Specimen 1322NC-1)

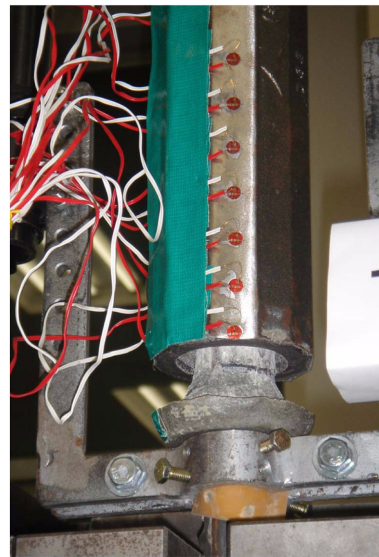


Fig. 6 Final failure pattern (Specimen 1355NM-1)

Stress is obtained from dividing the load on the specimens by the nominal sectional area of bar, and serial numbers show the attachment location of strain gauges on the surface of sleeves, as indicated by Fig. 3.

As Fig. 7 and Fig. 8 show, longitudinal strain in sleeve of the specimens 1322NC-1 and 1355NM-1 acted to the compression direction at the nearest location from sleeve end. However, it was small in the tensile direction at the surrounding of sleeve end, and increased until reaching sleeve near to the end of the embedded bar but decreased again when it passed this location. Longitudinal strain of each location increases almost in proportion to stress applied on the specimen before the embedded reinforcing bar yields, but after the bar starts to yield, it showed a tendency to increase rapidly inside the sleeve but reduced its rate of increase or decreased at sleeve end with a boundary where

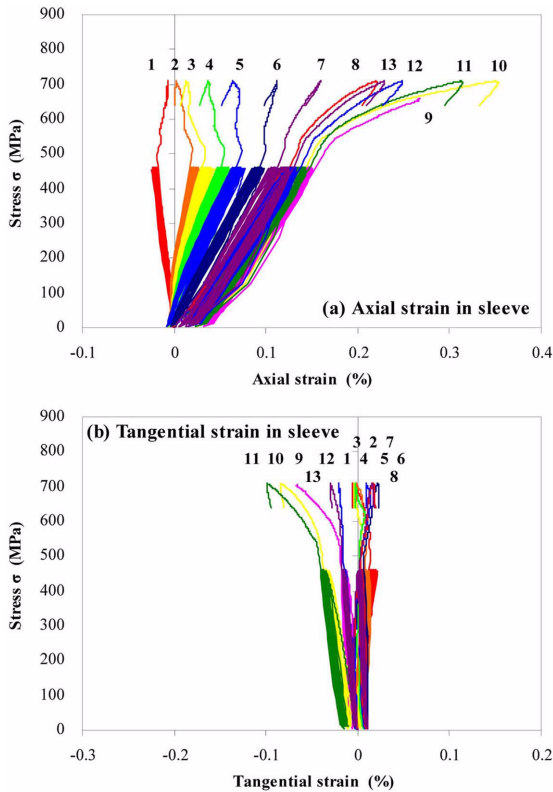


Fig. 7 Longitudinal and tangential strain distribution of specimen (1322NC-1)

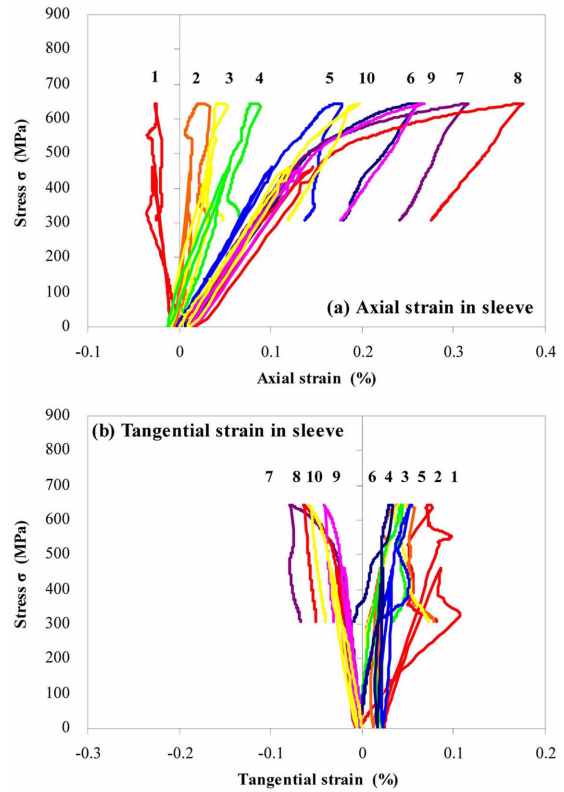


Fig. 8 Longitudinal and tangential strain distribution of specimen (1355NM-1)

the specimen 1322NC-1 is 4.7d distance from sleeve end, and the specimen 1355NM-1 is 2.8d distance from sleeve end. Tangential strain in sleeve was distributed to tensile direction at area of sleeve end but was distributed to compression direction inside sleeve with a boundary where the specimen 1322NC-1 is 4.7d distance from sleeve end and specimen 1355NM-1 is 2.8d distance from sleeve end.

When the stress acting on the two above specimens is at the same level, specimen 1355NM-1, for which development length of the bar is short, had relatively more longitudinal and tangential strain in the sleeve than the other specimen. Specimen 1322NC-1, on which cyclic loading test was carried out, showed longitudinal and tangential strain in sleeve by 30 times of cyclic loading within the elasticity range even less than 0.02%, so the overall effect of cyclic loading was not so high.

When maximum load acts to the aforementioned two specimens, the maximum longitudinal strain in sleeve was found to be 0.31% for specimen 1322NC-1 and 0.37% for specimen 1355NM-1 to tensile direction from sleeve near to end of embedded bar, while the maximum tangential strain in sleeve was 0.10% for specimen 1322NC and 0.08% for specimen 1355NM-1 to the compression direction from sleeve near to end of embedded bar. In addition, the other six specimens having other test variables showed a similar strain distribution and tendency within a small range of difference.

### 3. Bond strength considering lateral confining action of sleeve

#### 3.1 Evaluation on lateral confining pressure of sleeve

The mortar-filled sleeve reinforcing bar splice, in which stress is transferred to filled mortar through embedded bar, has a lateral confinement action that restricts splitting crack occurring in filled mortar by external sleeve. As Fig. 9 shows, lateral confining pressure of the sleeve  $f_{lat}$ , can be calculated using the equilibrium condition of the force occurring between filled mortar and sleeve as follows.

$$f_{lat} = \frac{2F_{sx}}{d_i \cdot \Delta l} = \frac{2\sigma_{sx} \cdot t_s \cdot \Delta l}{d_i \cdot \Delta l} = \frac{2\sigma_{sx} \cdot t_s}{d_i} \quad (1)$$

Where,  $F_{sx}$  is tangential force applying to unit length of sleeve,  $d_i$  is inside diameter of sleeve,  $\Delta l$  is unit length of sleeve,  $\sigma_{sx}$  is tangential stress applying to sleeve,  $t_s$  is thickness of sleeve.

Relation between stress and strain in sleeve can be derived through the following Eqs. (2) and (3), because stress in sleeve is both tangential and longitudinal. From these two equations, tangential stress ( $\sigma_{sx}$ ) can be determined as Eq. (4). When Eq. (4) is substituted to Eq. (1), lateral confining pressure of the sleeve  $f_{lat}$ , shall be presented as Eq. (5).

$$\varepsilon_{sx} = \frac{\sigma_{sx}}{E_{sx}} - \frac{\sigma_{sy}}{E_{sy}} \nu_{sy} \quad (2)$$

$$\varepsilon_{sy} = \frac{\sigma_{sy}}{E_{sy}} - \frac{\sigma_{sx}}{E_{sx}} \nu_{sx} \quad (3)$$

$$\sigma_{sx} = \frac{E_{sx}}{1 - \nu_{sx} \cdot \nu_{sy}} (\varepsilon_{sx} + \nu_{sy} \cdot \varepsilon_{sy}) \quad (4)$$

$$f_{lat} = \frac{2E_{sx}}{1 - \nu_{sx} \cdot \nu_{sy}} (\varepsilon_{sx} + \nu_{sy} \cdot \varepsilon_{sy}) \frac{t_s}{d_i} \quad (5)$$

Where,  $\varepsilon_{sx}$  is tangential strain in sleeve,  $\sigma_{sx}$  is tangential stress in sleeve,  $E_{sx}$  is tangential modulus of elasticity in sleeve,  $\sigma_{sy}$  is longitudinal stress in sleeve,  $E_{sy}$  is longitudinal modulus of elasticity in sleeve,  $\nu_{sy}$  is longitudinal Poisson's ratio in sleeve,  $\varepsilon_{sy}$  is longitudinal strain in sleeve,  $\nu_{sx}$  is

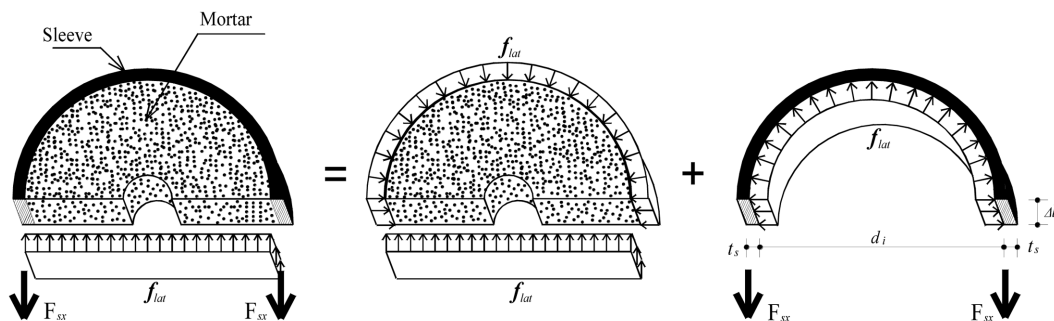


Fig. 9 Free body diagram of mortar-filled sleeve bar splice (Einea *et al.* 1995)

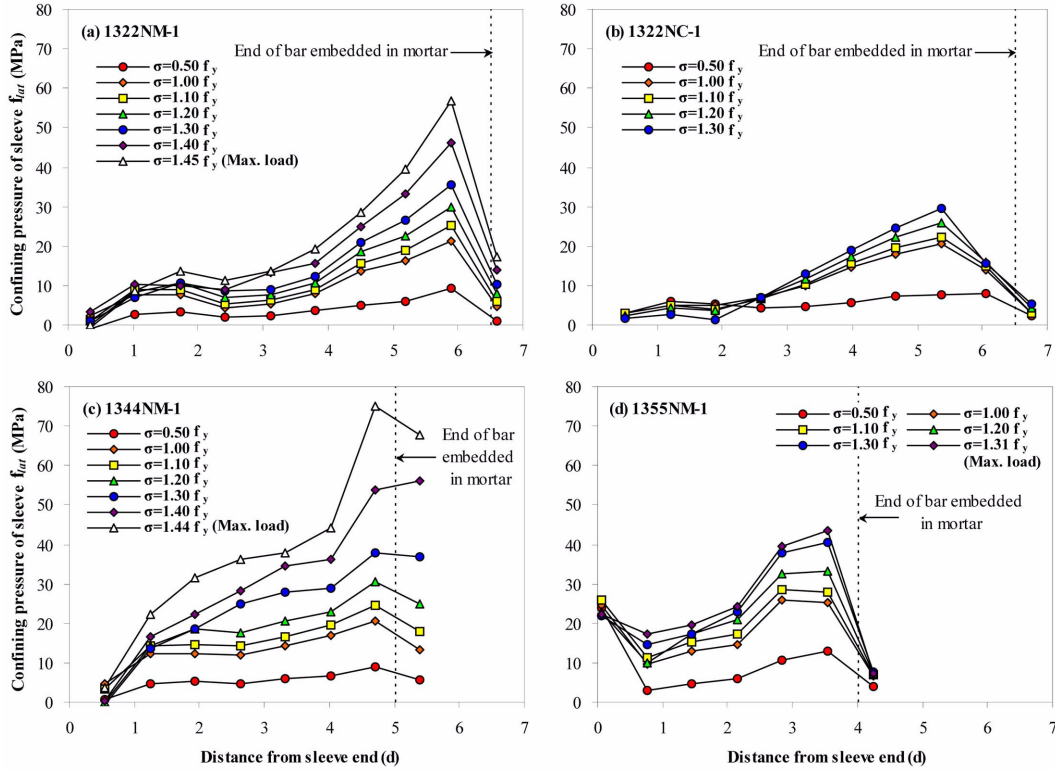


Fig. 10 Distribution of confining pressure by sleeve for each loading stage of representative specimens

tangential Poisson's ratio in sleeve

Fig. 10 shows the lateral confining pressure of the sleeves of four representative specimens with embedded D35 bar and N mortar through the calculation using Eq. (5) for each major stage. Fig. 11 compares the confinement pressure of each sleeve when the maximum load is applied on experimental specimens, where tangential modulus of elasticity in sleeve ( $E_{sx}$ ) used the result of material test, and longitudinal and tangential Poisson's ratio ( $\nu_{sy}$ ,  $\nu_{sx}$ ) was applied as 0.3. Tangential and longitudinal strain in sleeve ( $\epsilon_{sx}$ ,  $\epsilon_{sy}$ ) were determined from the two-direction strain gauge attached in a specified location on the sleeve surface.

As (a) and (b) of Fig. 10 show, confining pressure of specimens 1322NM-1 and 1322NC-1, where the development length of bar is  $6.5d$  and the bar was finally fractured, was not almost affected by loading methods. In these two specimens, when the stress level applied to reinforcing bar is within the range of elasticity, the difference in the confining pressure did not vary significantly according to the location of sleeve. However, as load on the specimens was increased, both showed a tendency to increase confining pressure rapidly at sleeve near to bar end rather than at sleeve end. Herein, specimen 1322NC-1, on which cyclic loading was tested, is estimated to show no significant difference from 1322NM-1, on which monotonic loading was tested, when comparing tendency of confining pressure distribution by loading stage, while it was difficult to identify the distribution of confinement pressure due to strain gauge failure at the stage where the maximum load was acted.

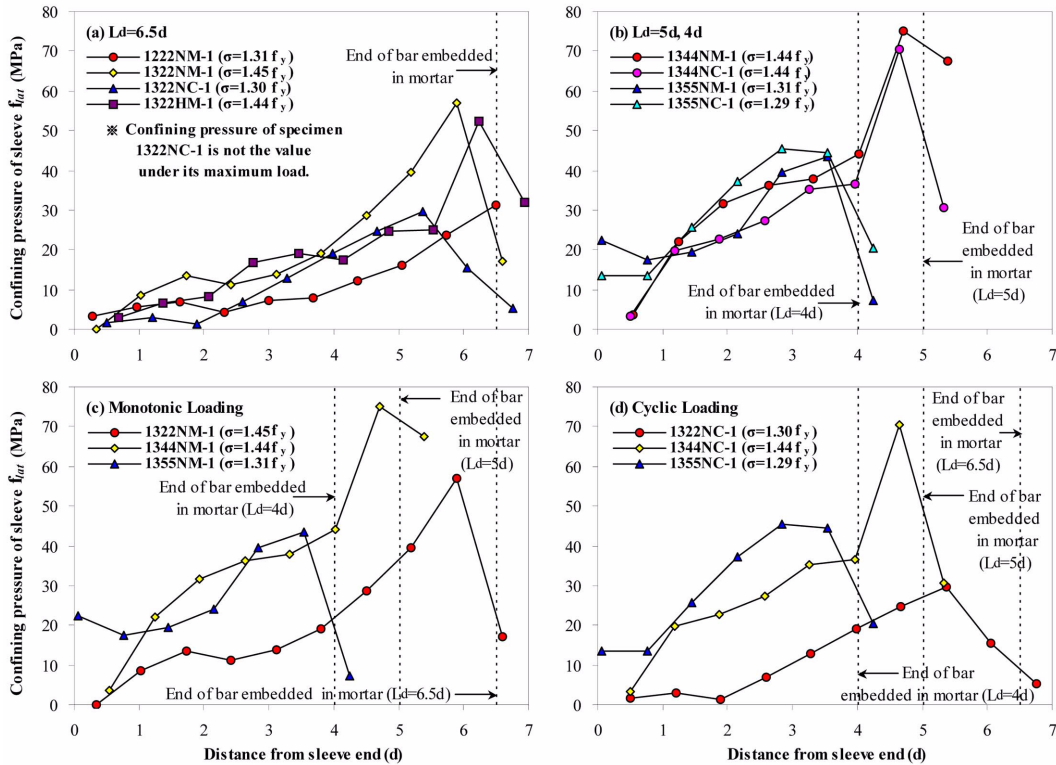


Fig. 11 Comparison of confining pressure of sleeve at maximum load

Unlike specimen 1322NM-1, where the development length of reinforcing bar was 6.5d and the bar was fractured, the confining pressure of specimen 1344NM-1 where the development length of bar was 5d and a final bond failure occurred, didn't show a big difference according to location of sleeve, even at the stage that the stress applied to bar exceeded its elasticity range, but rather showed a big relative value at location near to sleeve end. The confining pressure of the specimen 1344NM-1 was distributed relatively high in every location of sleeve compared to specimen 1322NM-1 when they both had maximum load. As (d) of Fig. 10 indicates, the confining pressure of specimen 1355NM-1, which had 4d development length of bar and a final bond failure, had a distribution similar to that of specimen 1344NM-1, which had 5d development length of bar and a final bond failure. But the confining pressure of this specimen showed a relatively large value at sleeve near to end of embedded bar from the low stress stage, and also showed a distribution of relatively high confining pressure at the same stress level.

(a) of Fig. 11 shows a comparison of confining pressures between three specimens which had 6.5d development length of bar and a final bar fracture at their maximum load. Here, there is no particular variation in their confining pressures depending on mortar strength, but a big difference in them depending on the size of embedded bar. Such differences may come from those in the shapes of sleeves according to size of the bar and the tensile strengths of the bars embedded in sleeve. When we see (b) of Fig. 11, confining pressures of four specimens which had 5d or 4d development length of bar and final bond failure at their maximum load were not affected by loading method but

showed a big difference in their distribution and intensity depending on development length of bar. As shown in (c) and (d) of Fig. 11, it can be shown that difference in the distribution and the intensity of confinement pressure was found according to development length of bar when considering the distribution of confining pressures of three specimens with same mortar and different development length of bar at their maximum load.

Of the specimens which had 6.5d development length of bar and final bar fracture, the maximum confining pressure acting on sleeve at the maximum load was shown to be 52~57MPa and 31MPa for the specimens with D35 and D25, respectively. And, of the specimens which had a final bond failure, the specimens with 5d and 4d development length of bar showed 71~75MPa and 43~46MPa, respectively.

### 3.2 Bond strength considering lateral confining action in sleeve

By applying the equation for bond strength between deformed bar and concrete presented by Untrauer and Henry (1965), which reflects lateral confining action to the mortar-filled sleeve reinforcing bar splice by converting it to SI unit, the bond stress between embedded bar and filled mortar can be calculated by the following equation.

$$\tau = (1.49 + 0.45\sqrt{f_{lat}})\sqrt{f_m} \quad (6)$$

Where,  $\tau$  is bond stress between the embedded bar and the filled mortar in the mortar-filled sleeve bar splice (MPa),  $f_{lat}$  is lateral confining pressure by sleeve (MPa),  $f_m$  is compressive strength of filled mortar (MPa).

Fig. 12 illustrates the calculated bond stress of mortar-filled sleeve bar splice of eight specimens applying the result of lateral confining pressure by sleeve at their maximum load to Eq. (6). From Fig. 12, we can identify that the lateral confinement action by sleeve increased bond stress between bar and mortar by maximum 2.7~3.4 times for specimens that had a bar fracture, and by maximum 3.0~3.6 times for specimens that had a bond failure. Tables 6 and 7 indicate the maximum experimental strength value and the calculated value of the bond strength of four specimens that had a final bond failure and four specimens that had a final bar fracture at their maximum load, respectively. Thus, the calculated value ( $P_{b.cal}$ ) of bond strength of eight specimens was derived from following equation.

$$P_{b.cal} = \pi d \left[ \tau_1 \left( \frac{l_1 + l_2}{2} \right) + \sum_{i=2}^{n-1} \tau_i \left( \frac{l_{i+1} - l_{i-1}}{2} \right) + \tau_n \left( L_d - \frac{l_n + l_{n-1}}{2} \right) \right] \quad (7)$$

Where,  $d$  is nominal diameter of embedded bar in sleeve (mm),  $\tau_i$  is bond stress of sleeve splice calculated by the above Eq. (6) from strain gauge attached at location "i" of specimens (MPa),  $l_i$  is distance from sleeve end to strain gauge at location "i" (mm),  $n$  is the first location of strain gauge passing development length of bar embedded in sleeve,  $L_d$  is development length of bar embedded in sleeve (mm).

By using the equation of bond strength as presented by Untrauer and Henry, Table 6 compares bond strength between bar and mortar of four specimens which had a final bond failure with the maximum experimental strength of this specimen. Herein, the bond strength was calculated in

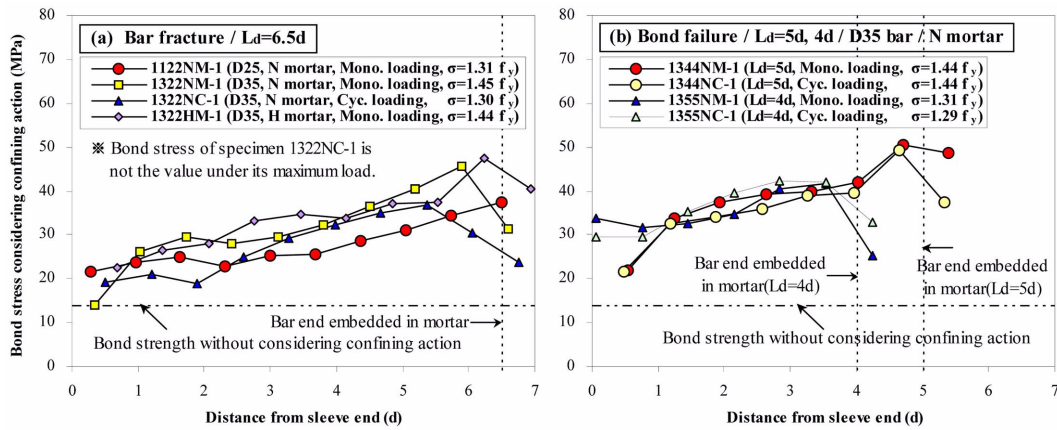


Fig. 12 Comparison of bond stress considering confinement action under maximum load

Table 6 Comparison between maximum experimental strength value and calculated value of bond strength for specimens which had a bond failure

Specimen	Experimental value $P_{test}$ (kN)	Calculated value $P_{b,cal}$ (kN)	$P_{test}/P_{b,cal}$
1344NM-1	677.9	709.8	0.955
1344NC-1	677.9	674.4	1.005
1355NM-1	616.6	538.9	1.144
1355NC-1	607.7	559.7	1.086
Average			1.048
Coefficient of variation			0.080

consideration of the lateral confining action of sleeve. In Table 6, the maximum strength of four specimens which had a final bond failure were also estimated within 5% average error, and coefficient variation of these specimens was found to be 8.0%. And the experimental value of specimen 1355NM-1 which showed the biggest error could be estimated within 15% average error. However, the above method of calculating bond strength showed a tendency to underestimate the experimental value as development length of bar becomes shorter. When bond strength of this splice was estimated after reflecting confinement action of sleeve for four specimens which had a bar fracture as explained above, it was found to exceed maximum strength of specimens by an average of 14%, as shown in Table 7. For these four bar fractured specimens, it is understood that bond strength between bar and mortar in these specimens is relatively larger than bar fracture strength, as the calculated result in Table 7 shows, which may be the reason the bar fracture occurred prior to the bond failure.

Table 7 Comparison between maximum experimental strength value and calculated value of bond strength for specimens which had a bar fracture

Specimen	Experimental value $P_{test}$ (kN)	Calculated value $P_{b,cal}$ (kN)	$P_{test}/P_{b,cal}$
1122NM-1	325.2	358.0	0.908
1322NM-1	679.8	778.6	0.873
1322NC-1	610.8	675.3	0.904
1322HM-1	676.4	809.1	0.836
Average			0.880

#### 4. Conclusions

In this study, an experiment of monotonic loading and cyclic loading was conducted with a full-sized mortar filled sleeve reinforcing bar splice embedding D35 and D25 bar attaching two-direction strain gauges on the surface of sleeve with experimental variables such as development length of bar, etc. Based on the results of this experiment, we analyzed and studied the influence of lateral confining action by sleeve on bond strength between bar and mortar to reach the following conclusion.

1. The confining pressure acting on mortar-filled sleeve bar splice estimated using the measured longitudinal and tangential strain in sleeve was indicated to be maximum 31~75 MPa, and it was shown that this confining pressure differs depending on the development length and size of bar.
2. The method used to evaluate bond strength between bar and mortar of mortar-filled sleeve bar splice was in good agreement with the results of the experiment in which bond failure occurred by applying lateral confining action to the equation of bond strength suggested by Untauer and Henry.
3. When applying confining pressure by sleeve of this experiment to the equation to determine bond strength suggested by Untauer and Henry, bond strength between bar and filled mortar was found to increase by maximum 3.0~3.6 times for specimens which had a bond failure, and by maximum 2.7~3.4 times for specimens which had a bar fracture due to lateral confining action by sleeve.

#### References

- Ahn, B.K., Kim, H.K. and Park, B.M. (2003) "Confining effect of mortar grouted splice sleeve on reinforcing bar", *J. Korea Concrete Institute*, **15**(1), 102-109. (in Korean)
- Ase, M. *et al.* (1996) "Study for practical application of grout filled connectors for high strength reinforcing bars (No. 1 performance of the grout filled connector with SD490 reinforcing bars)", *Summaries of Technical Papers of Annual Meeting Architectural Institute of Japan*, C-2, Structures IV, 743-744. (in Japanese)
- Bing, L., Park, B. and Tanaka, H. (2001) "Stress-strain behavior of high-strength concrete confined by ultra-high- and normal-strength transverse reinforcements", *ACI Struct. J.*, **98**(3), 395-406.
- Choi, Y.H., Kim, K.S. and Choi, S.M. (2008) "Simplified P-M interaction curve for square steel tube filled with high-strength concrete", *Thin Wall. Struct.*, **46**(2008), 506-515.
- Cusson, D. and Paultre, P. (1994) "High-strength concrete columns confined by rectangular ties", *J. Struct. Eng.*,

- ASCE, **120**(3), 783-804.
- Cusson, D. and Paultre, P. (1995) "Stress-strain model for confined high-strength concrete", *J. Struct. Eng.*, ASCE, **121**(3), 468-477
- Einea, A., Yamane, T. and Tadros, M.K. (1995) "Grout-filled pipe splices for precast concrete construction", *PCI J.*, **40**(1), 82-93.
- Kilpatrick, A.E. and Rangan, B.V. (1999) "Tests on high-strength concrete-filled steel tubular columns", *ACI Struct. J.*, **96**(2), 268-274.
- Kim, H.K. (2008) "Structural performance of steel pipe splice for SD500 high-strength reinforcing bar under cyclic loading", *Architect. Res.*, **10**(1), 13-23.
- Kim, H.K. (2008) "Confining effect of mortar-filled steel pipe splice", *Architect. Res.*, **10**(2), 27-35.
- Liang, Q.Q. (2009) "Strength and ductility of high strength concrete-filled steel tubular beam-columns", *J. Constr. Steel Res.*, **65**, 687-698.
- Liu, D. (2006) "Behaviour of eccentrically loaded high-strength rectangular concrete-filled steel tubular columns", *J. Constr. Steel Res.*, **62**, 839-846.
- Liu, D. and Gho, W.L. (2005) "Axial load behaviour of high-strength rectangular concrete-filled steel tubular stub columns", *Thin Wal. Struct.*, **43**, 1131-1142.
- Lue, D.M., Liu, J.L. and Yen, T. (2007) "Experimental study on rectangular CFT columns with high-strength concrete", *J. Constr. Steel Res.*, **63**, 37-44.
- Mander, J.B., Priestley, J.N. and Park, R. (1988) "Theoretical stress-strain model for confined concrete", *J. Struct. Eng.*, ASCE, **114**(8), 1804-1826.
- Mirmiran, A. and Shahawy, M. (1997) "Behavior of concrete columns confined by fiber composites", *J. Struct. Eng.*, ASCE, **123**(5), 583-590.
- Orangun, C.O., Jirsa, J.O. and Breen, J.E. (1977) "A reevaluation of test data on development length and splices", *ACI J.*, **74**(3), 114-122.
- Park, J.W., Hong, Y.K. and Choi, S.M. (2010) "Behaviors of concrete filled square steel tubes confined by carbon fiber sheets (CFS) under compression and cyclic loads", *Steel Compos. Struct.*, **10**(2), 187-205.
- Razvi, S.R. and Saatcioglu, M. (1999) "Confinement model for high-strength concrete", *J. Struct. Eng.*, ASCE, **125**(3), 281-289.
- Saadatmanesh, H., Ehsani, M.R. and Li, M.W. (1994) "Strength and ductility of concrete columns externally reinforced with fiber composite straps", *ACI Struct. J.*, **91**(4), 434-447.
- Saatcioglu, M. and Razvi, S.R. (1992) "Strength and ductility of confined concrete", *J. Struct. Eng.*, ASCE, **118**(6), 1590-1607.
- Saatcioglu, M. and Razvi, S.R. (1998) "High-strength concrete columns with square sections under concentric compression", *J. Struct. Eng.*, ASCE, **124**(12), 1438-1447.
- Soroushian, P., Choi, K.B., Park, G.H. and Aslani, F. (1991) "Bond of deformed bars to concrete: effects of confinement and strength of concrete", *ACI Mater. J.*, **88**(3), 227-232.
- Tao, Z., Han, L.H. and Wang, L.L. (2007) "Compressive and flexural behaviour of CFRP-repaired concrete-filled steel tubes after exposure to fire", *J. Constr. Steel Res.*, **63**, 1116-1126.
- Untrauer, R.E. and Henry, R.L. (1965) "Influence of normal pressure on bond strength", *ACI J.*, **62**(5), 577-585
- Xiao, Y., He, W. and Choi, K.K. (2005) "Confined concrete-filled tubular columns", *J. Struct. Eng.*, ASCE, **131**(3), 488-497.